Carbohydrate Polymers 77 (2009) 449–456

Contents lists available at ScienceDirect

Carbohydrate Polymers

journal homepage: www.elsevier.com/locate/carbpol

A novel biopolymer/rectorite nanocomposite with antimicrobial activity

Xiaoying Wang [a,b,*], Yumin Du [a,*], Jiwen Luo [a], Jianhong Yang [a], Weiping Wang [a], John F. Kennedy [c]

[a] Department of Environmental Science, College of Resource and Environmental Science, Wuhan University, Wuhan 430079, China
[b] State Key Laboratory of Pulp and Paper Engineering, School of Light Industry and Food, South China University of Technology, Guangzhou 510640, People's Republic of China
[c] Birmingham Carbohydrate and Protein Technology Group, Chembiotech Laboratories, University of Birmingham Research Park, Vincent Drive, Birmingham B15 2SQ, UK

ARTICLE INFO

Article history:
Received 2 May 2008
Received in revised form 11 September 2008
Accepted 16 January 2009
Available online 29 January 2009

Keywords:
HTCC
Rectorite
Nanocomposite
Antimicrobial activity

ABSTRACT

Rectorite (REC), a type of layered silicate, was used to prepare the intercalated nanocomposites with quaternized chitosan (HTCC). Characterization by XRD and TEM revealed that HTCC were intercalated into the intergallery of REC. Moreover, it was confirmed from FT-IR, XRD and ζ-potential analyses that interaction between HTCC and REC took place. Two *in vitro* antimicrobial assays indicated that all the nanocomposites exhibited strong inhibition against Gram-positive bacteria, Gram-negative bacteria and Fungi under weak acid, water and weak basic condition, particularly against Gram-positive bacteria. Moreover, with increasing the amount or the interlayer distance of organic REC, the antimicrobial activity was stronger. The lowest minimum inhibition concentration values of the nanocomposites against *Staphylococcus aureus* and *Bacillus subtilis* were less than 0.00313% (w/v) in all media tested, and the killing rate on *S. aureus* reached more than 90% in 30 min. The mechanism of the antimicrobial action was briefly discussed.

1. Introduction

Antimicrobial agents can be divided into inorganic and organic ones according to their chemical composition. Inorganic antimicrobial agents show long life expectancy and high heat resistance; however, they exhibit weak mould proof activity and large dosage are needed when used, etc., (Guo, Ma, Guo, & Xu, 2005; Zhou, Xia, Ye, & Hu, 2004). While organic antibacterial agents show good inhibition efficiency and a broad spectrum of activity, more importantly they display blending compatibility with organic matrixes such as textile, paints, polymer, etc., however, their relative low stability (e.g., low decomposition temperature and short life expectancy) cannot be ignored (Suci, Vrany, & Mittelman, 1998). As a result, there is urgent need to develop organic–inorganic hybrid materials provided with dual antibacterial advantages of organic antimicrobial agents and inorganic antimicrobial agents as they will become more important in the antimicrobial material market. From this point of view, it is noteworthy to point out the polymer/layered silicate nanocomposites (PLNs) technology, which provide an attractive way to develop new organic–inorganic hybrid materials with properties that are inherent to both types of components.

Rectorite (REC) is a type of layered silicate which has been studied in the PLNs technology in recent years; the structure is similar to montmorillonite (MMT) where most work on PLNs has been concentrated. At the same time, REC also shows adsorption capacity on bacteria and immobilization activity of cell toxin (Zhang, Zhang, & Yu, 2003), which is also similar to MMT (Guo et al., 2005; Herrera, Burghardt, & Phillips, 2000). Modified layered silicates could adsorb both natural and anthropogenic toxin, and exhibited an inhibitory property for the proliferation of bacteria (Guo et al., 2005; Lemke, Grant, & Phillips, 1998). However, there are only several reports about polymer/layered silicate nanocomposites with antibacterial activity, our previous paper reported the good antibacterial activity of chitosan/rectorite nanocomposites (Wang et al., 2006), and Rhim et al. reported the chitosan/clay nanocomposite films with antimicrobial activity (Rhim, Hong, Park, & Ng, 2006).

Chitosan (CS) is the second most abundant polysaccharide in nature, it has been shown to be useful in many different applications; one of them is as a natural antimicrobial agent. CS has advantages over other type of disinfectants because of its higher antibacterial activity, a broader spectrum of activity, a higher killing rate and a lower toxicity towards mammalian cells (Shahidi, Arachchi, & Jeon, 1999). Despite all these advantages, chitosan *per se* lacks good solubility above pH 6.5; its applications in a commercial context are not as wide as expected. Accordingly, CS/REC nanocomposites may be not applied widely (Wang et al., 2006). Therefore, it is very necessary to prepare functional chitosan derivative in attempt to increase its solubility in water and thereby to broaden its applications. N-(2-hydroxyl) propyl-3-trimethyl ammonium chitosan chloride (HTCC) is just the derivative soluble

* Corresponding authors. Tel.: +86 27 68778501, +86 20 31 325809;+fax: +86 27 68778501.
E-mail addresses: xyw@scut.edu.cn (X. Wang), duyumin@whu.edu.cn (Y. Du).

0144-8617/$ - see front matter © 2009 Elsevier Ltd. All rights reserved.
doi:10.1016/j.carbpol.2009.01.015

in a wide pH range; it can be prepared by a relatively easy chemical reaction of CS and glycidyl-trimethyl-ammonium chloride (GTMAC) (Li, Du, Xu, & Zhan, 2004). There are more advantages in HTCC than in CS. First, it is water-soluble and thus the intercalation between HTCC and REC can proceed in mild condition—water, which does not include organic solvent. In addition, HTCC shows higher positive charge density than pure CS (Qin et al., 2004), so in the intercalation technology, it is easier to intercalate into the interlayer of silicate. And compared to pure CS, HTCC can inhibit the growth of bacteria in acid, water and base solution while CS only show antibacterial activity in acid solution (Qin et al., 2004). Besides, HTCC is potential to be used as an absorption enhancer across intestinal epithelial due to its mucoadhesive and permeability enhancing property; it is very suitable for biomedical application (Kotzle et al., 1999). Therefore, HTCC/layered silicate nanocomposites will have more potential applications than CS/layered silicate nanocomposites.

The focus of this paper is on preparing biopolymer/rectorite nanocomposites based on HTCC; it appears as an improved way of developing a novel PLNs nanocomposite which can inhibit the growth of bacteria in a wide pH range, and it is very favorable to the application of PLNs. First, according to our previous study (Wang et al., 2006), organic rectorite(OREC) was prepared. Then, HTCC/OREC nanocomposites with different mass ratios of HTCC to OREC were prepared. XRD and TEM were used to characterize their structures. FT-IR, XRD and ζ-potential analyses confirmed the interaction between HTCC and REC. At last, this paper detailed antimicrobial activity of HTCC/OREC nanocomposites.

2. Experimental

2.1. Materials

Chitosan (CS) from a shrimp shell was purchased from Yuhuan Ocean Biochemical Co. (Taizhou, China). The degree of deacetylation was 92% (determined by elemental analysis) (Xu, McCarthy, & Gross, 1996) and its weight average molecular weight (M_w) was 2.1×10^5 (determined by GPC method) (Qin, Du, & Xiao, 2002). Calcium rectorite (Ca^{2+}-REC) refined from the clay minerals was provided by Hubei Mingliu Inc., Co. (Wuhan, China). Cetyltrimethyl ammonium bromide (CTAB) was supplied by Xinrui Science and Technology Inc., Co. (Wuhan, China). All other chemicals were of analytical grade.

2.2. Synthesis of quaternized chitosan

N-(2-hydroxyl) propyl-3-trimethyl ammonium chitosan chloride (HTCC) was prepared as shown in Scheme 1 according to reference (Li et al., 2004). About 0.5 mol of concentrated hydrochloric acid was dropped into the solution of trimethylamine (0.5 mol) at 4 °C. After stirring for about 10 min, 0.42 mol of epoxy chloropropane were added into the resulting solution at 35 °C. After homogenization, the mixing solution was heated to 54 °C, and was then trickled slowly by aqueous NaOH solution (50 ml 40 wt %). The addition of NaOH was performed within 1–1.5 h, after another 2 h of stirring, the reaction mixture was refined by vacuum distillation at 40 °C for 20 min, then intermediate for the preparation of HTCC———2,3-epoxypropyltrimethyl ammonium chloride (EPTMAC) was obtained. Subsequently, 12 g of chitosan was dispersed in EPTMAC solution after which was adjusted to pH 9 and was stirred at 75 °C for 6 h. Then the reaction mixture was dialyzed, precipitated by acetone, and finally vacuum-dried to obtain HTCC. Its M_w was 1.08×10^5 (determined by GPC method) and the degree of substitution (DS) was 82% (determined by potentiometry) (Li et al., 2004).

2.3. Preparation of HTCC/OREC nanocomposites

Organic rectorite (OREC) was prepared according to our previous work (Wang et al., 2006). eparation of HTCC/OREC nanocomposites was as follows: HTCC was dissolved in water to obtain the 0.5% (w/v) solution. The resulting solution was added slowly into the pretreated OREC suspension under stirring at 80 °C to obtain the nanocomposites with initial HTCC/OREC weight ratios of 1:1, 2:1, 4:1. The resulting mixture was agitated for 2 days. Finally the nanocomposites were freeze-dried at −50 °C and ground to powder. A conceptual illustration of the intercalation of HTCC into REC is shown in Scheme 2. Firstly, quaternary alkylammonium (CTAB) cations enter into the interlayer of rectorite by ion-exchange reactions, the alkyl chains arrange orderly between the interlayer because of cation strong interaction (Vaia, Teukolsky, & Giannelis, 1994). In this way, the normally hydrophilic silicate surface is converted to an organophilic one, making the intercalation of polymers easier. Therefore, after that, quternized chitosan (HTCC) can intercalate into the clay gallery in the help of agitation action and the interaction between HTCC and CTAB chains (Ray & Okamoto, 2003).

2.4. Characterization

The X-ray diffraction (XRD) experiment was performed using a D8 Advance diffractometer (Bruker, USA) with Cu target and Kα radiation ($\lambda = 0.154$ nm) at 40 KV and 50 mA. The scanning rate was 0.5°/min and the scanning scope of 2θ was 1°–10° and 5°–45° in a fixed time mode with a step interval of 0.02° at room temperature.

Ultrathin films for transmission electron microscopy (TEM) were prepared by cutting from the epoxy block with the embedded nanocomposites sheet at room temperature using an LKB-8800 ultratome. The TEM micrographs were taken using a transmittance electron microscope [JEM-2010 FEF (UHR), JEOL, Japan] at an accelerating voltage of 200 KV.

FT-IR spectra were recorded in KBr pellets on a Nicolet FT-IR 5700 spectrophotometer (Madison, USA) by the method of transmission.

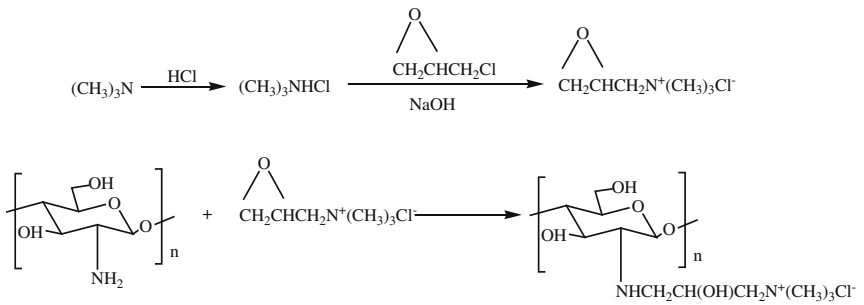

Scheme 1. Preparation of HTCC.

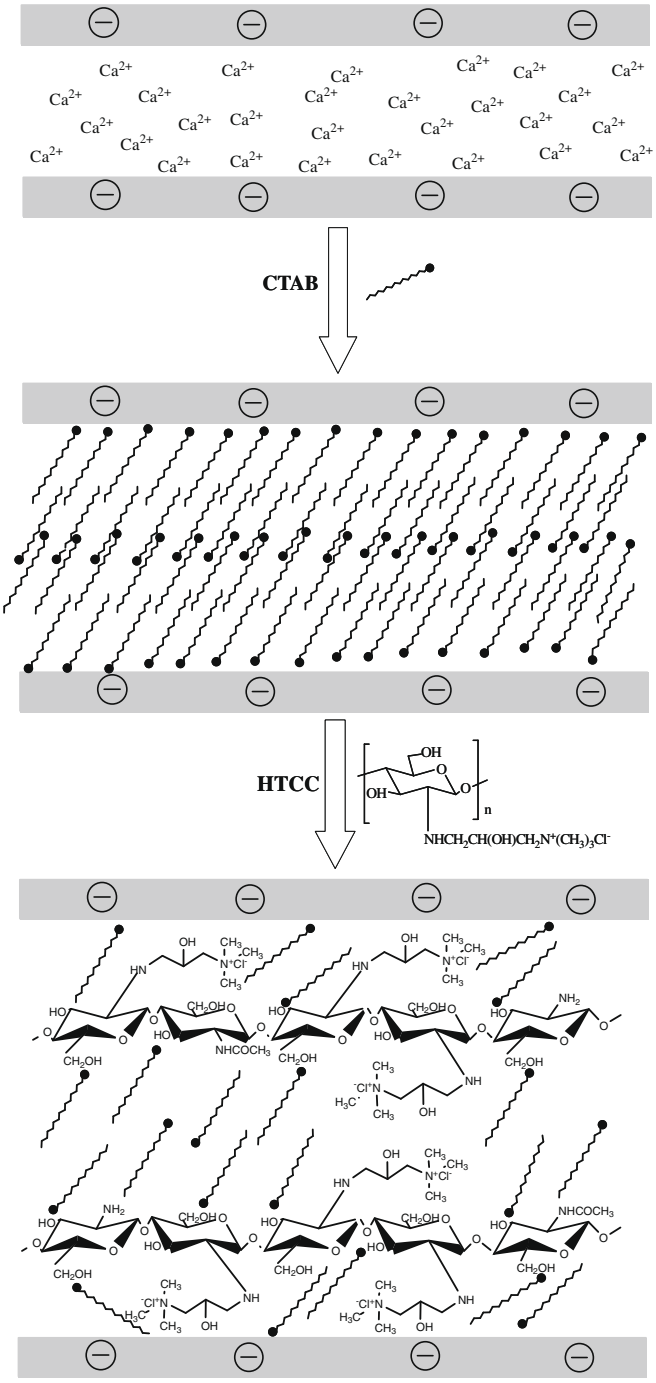

Scheme 2. Intercalation of HTCC into REC.

The pH values of the HTCC/OREC nanocomposite suspension were obtained by using a pH analyzer (Lida, pHS-25, China). ζ-potential analysis was carried out on a Zetasizer 3000HSA apparatus (Malven, England). The suspensions for the pH value and ζ-potential analyses were prepared through a process as the preparation of the HTCC/OREC nanocomposites. In this case, the concentration of the nanocomposites in aqueous suspension was fixed to be 0.1% (w/v).

2.5. Antibacterial assays

Gram-positive bacteria *Staphylococcus aureus*, *Bacillus subtilis*, Gram-negative bacteria *Escherichia coli, Pseudomonas aeruginosa* and Fungi *Aspergillus niveus* were provided by China center for Type Culture Collection (CCTCC at Wuhan University) and incubated on nutrient agar (peptone 1%, beef extract 0.5%, NaCl 0.5%, agar 2%, pH 7.2).

2.5.1. Determination of the minimum inhibition concentration (MIC)

The antibacterial activities of the nanocomposites were evaluated by finding the minimum inhibition concentration (MIC) as the follows: the microorganism suspension was adjusted by 0.9% (w/v) sterile saline water to 10^5–10^6 CFU/ml. The nanocomposites, HTCC, REC and OREC solutions were prepared, respectively, in acetate buffer (pH 5.4), in water and in NaOH solution (pH 8.0) at a concentration of 1% (w/v). The resulting solutions and the nutrient agar were autoclaved at 121 °C for 20 min. The twofold serial dilutions (1 ml) of each sample were added to 9 ml nutrient agar for the final concentrations of 0.1% (w/v), 0.05% (w/v), 0.025% (w/v), 0.0125% (w/v), 0.00625% (w/v) and 0.00313% (w/v), the mixture were added into sterile Petri-dishes after completely mixing. A loop of each microorganism suspension was inoculated on cooled nutrient medium by means of drawing a stripe. The bacteria were cultured at 37 °C. MICs values were read after a 24 h of culture. The experiments were done for three times.

The minimum inhibition concentration (MIC) was defined as the lowest concentration required inhibiting the growth of bacteria, i.e. the concentration at which no microorganism colony or less than 5 colonies were visible within 19–38 h (Wang et al., 2006).

2.5.2. Determination of the killing rate

The bactericidal activity of CS was measured by enumeration of viable organisms, as previously described (Wang et al., 2006). The microorganism suspension was diluted by 0.9% (w/v) sterile saline water to ~10^4 CFU/ml. 1 ml of the cell suspension was added to 4 ml 0.5% HTCC/OREC nanocomposites, HTCC, REC and OREC aqueous solutions that had been autoclaved at 121 °C for 20 min. Another tubes without samples served as the control. Samples were removed after 5, 30, 60, 120, and 180 min, respectively. A 50 μl aliquot or the dilutions were spread on nutrient agar plates, which were incubated at 37 °C for 24 h, and the numbers of colonies were counted. The percent reductions in plate colonies were calculated by comparing the experiment plates to the control. All the data were the means from at least 3 parallel experiments that discrepancies among them were less than 5%.

2.5.3. Transmission electron microscopy for bacteria

Bacteria were prepared for transmission electron microscopy (TEM) as previously described (Helander, Nurmiaho-Lassila, Ahvenainen, Rhoades, & Roller, 2001; Liu, Du, Wang, & Sun, 2004). *E. coli* and *S. aureus* were grown in nutrient broth to obtain a culture with optical absorbance at 630 nm of 0.4. 1 ml of each culture was centrifuged at 11,000*g* for 10 min. The resulting pellet was resuspended in 0.1 M sodium phosphate buffer containing 0.85% sodium chloride, pH 7.2 (PBS). This suspension was supplemented with 1:1 HTCC/OREC nanocomposite with final concentration of 0.05% (w/v); the control suspension remained without supplement. After incubating for 20 min at 37 °C, the suspensions were centrifuged at 11,000*g*; the resulting pellets were washed twice with 0.1 M PBS and then were fixed with 2.5% glutaraldehyde in 0.1 M PBS. Specimens were prepared for electron microscopy by post-fixing with1% (w/v) OsO4 in 0.1 M PBS for 2 h at room temperature, washing once with the same buffer, dehydrating in a graded series of ethanol, washing with acetone and embedding in Spur low-viscosity medium. Thin sections of the specimens were cut with a diamond knife on an Ultracut Ultramicrotome (Super Nova; Reichert-Jung Optische Werke, Wien, Austria) and the sections were double-stained with saturated uranyl acetate and lead citrate. The grids were examined with an H-7000FA transmission

electron microscope (Hitachi, Tokyo, Japan) at an operating voltage of 75 kV.

3. Results and discussion

3.1. Structure and morphology

Fig. 1 represents XRD patterns of REC, OREC and corresponding nanocomposites. The d_{001} peak of OREC shifts towards lower angle in comparison with REC, and its Δd_L value (the interlayer distance) is 2.94 nm as calculated by Bragg's equation. This increase of the interlayer distance is a direct evidence of CTAB intercalated into the REC interlayer (Wang et al., 2006). In the same way, the interlayer distances of HTCC/OREC nanocomposites were enlarged to 4.56 nm, 4.8 nm and 4.48 nm, respectively. These results also prove that HTCC entered the intergallery space of clay and the corresponding nanocomposites were successfully prepared, as shown in Scheme 2. In other cases, it is noted that the interlayer distance of the nanocomposites was not proportional to the amount of OREC, which is in accordance with our previous report (Wang et al., 2006). In this system, the better intercalation was achieved when the mass ratio of HTCC and OREC was 2:1.

Direct evidence of this nanometer-scale dispersion of intercalated REC can be found in the transmission electron microscopy of the cross section of HTCC/OREC nanocomposite, as exhibited in Fig. 2 in two levels of magnification. The dark lines correspond to clay layers while the bright areas represent the HTCC matrix. Some large intercalated tactoids (multiplayer particles) are visible in the TEM images in low magnification (Fig. 2A), but these tactoids are dispersed uniformly in HTCC matrix despite the high content of clay (33 wt %). This fact clearly implies the high affinity between HTCC and OREC. An observation in high magnification (Fig. 2B) reveals that most of silicate particles still maintained the layered structure, and the Δd_L value of 4.8 nm can be measured in TEM images, which agrees with the XRD analysis. Interestingly, some highly delaminated structures are observed. In this case, the clays are exfoliated into slim slices with 2–4 layers, and even into single layer, which clearly demonstrates the better intercalation effeciency of 2:1 HTCC/OREC nanocomposite.

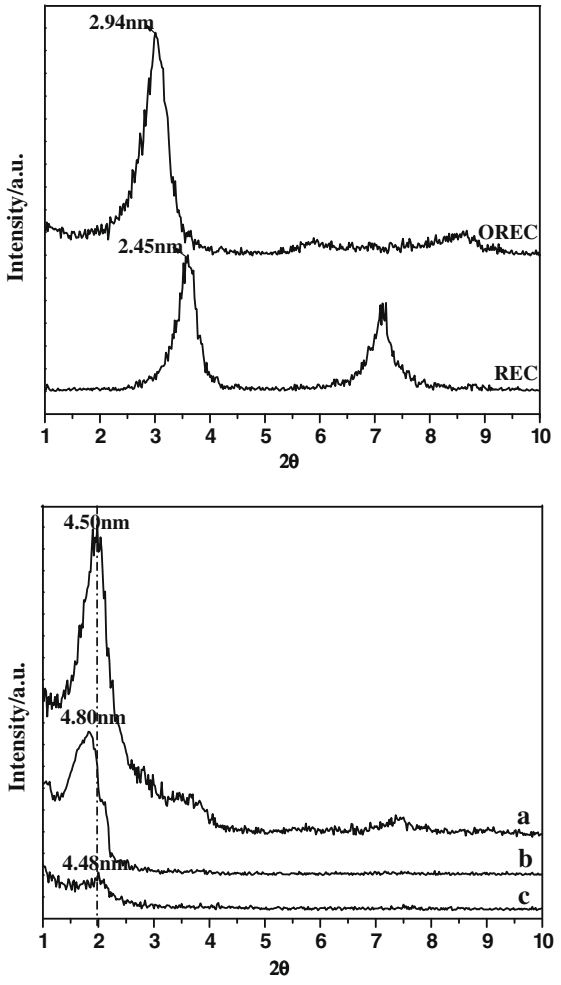

Fig. 1. XRD patterns of REC, OREC and nanocomposites with different HTCC/OREC ratios (a) 1:1, (b) 2: 1 and (c) 4: 1.

3.2. Interaction between HTCC and REC

Table 1 shows the pH values of REC, OREC, HTCC and the HTCC/OREC suspensions. The pH values of pure REC and HTCC are 7.27 and 6.58, respectively, while the pH values of the HTCC/OREC suspensions slowly increased from 6.14 to 6.50 as the REC content increased from 25 wt % to 50 wt %. Besides, Table 1 shows the ζ-potential value of REC, OREC, HTCC and the HTCC/OREC suspensions. Pure HTCC and REC particles exhibit ζ-potential value of +66.06 mV and −15.84 mV, respectively. And the ζ-potential values of the HTCC/OREC particles are positive, however, they are lower than that of pure HTCC. And obviously the ζ-potential value is not caused by the change of pH value. So this is the proof that the REC layers were covered by the HTCC molecules, and the existence of the electrostatic interaction between HTCC and REC (Chen & Zhang, 2006).

FT-IR spectra of REC, OREC, HTCC and HTCC/OREC nanocomposites are shown in Fig. 3. It can be observed that the spectra of the nanocomposites are good combination of the spectrum of HTCC with that of OREC. However, there are also distinct differences between them. Peaks between 3750–3000 cm^{-1} become stronger and wider, and even the vibration band at 3430 cm^{-1} in HTCC which attachs to N–H bonded to O-H shifts towards lower frequency, this is a strong proof of hydrogen bonding between –OH group in REC and –NH– and –OH groups in HTCC (Chen & Zhang, 2006; Darder, Colilla, & Ruiz-Hitzky, 2003; Wang et al., 2006). Besides, hydrogen bonding may take place between the HTCC molecules and inside the HTCC molecules, and it was reported that –OH groups in REC surface were able to interact immensely with the polymer substrate to form new interface layer or partly network structure (Wang et al., 2006). All the above analyses suggest that strong interaction between HTCC and silicates takes place.

Fig. 4 presents the X-ray diffraction of HTCC, OREC and HTCC/OREC nanocomposites. HTCC appears one major crystalline peak near 20° while the diffraction of OREC consist of five crystalline peaks at 7.1°, 18.2°, 19.8°, 22.0° and 36.4°. Compared to HTCC and OREC, the diffraction heights of the nanocomposites are gradually reduced. It reveals that the crystallization of both OREC and HTCC were destroyed, the reason may be that the molecular movement of HTCC chains is limited greatly because of the formation of the interaction structure.

Based upon these evidences, it is clearly demonstrated that HTCC strongly interacted with silicate and intercalated into the interlayer of silicate, the expected HTCC/OREC nanocomposites formed.

3.3. Antimicrobial activity

As shown in Tables 2 and 3, pure REC can not inhibit the growth of microbes whereas OREC shows slight antimicrobial activity. In addition, HTCC also shows a certain inhibitory effect on microorganisms, all HTCC/OREC nanocomposites exhibit strong antimicro-

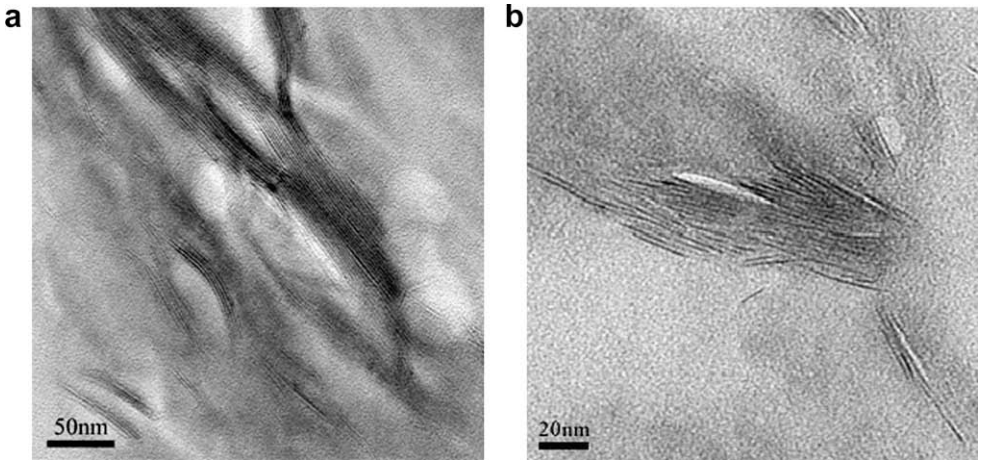

Fig. 2. TEM micrographs of nanocomposites with HTCC/OREC mass ratio of 2: 1.

Table 1
pH value and ζ-potential (mV) of HTCC, REC, OREC and nanocomposites with different HTCC/OREC ratios of (a) 1:1, (b) 2:1, and (c) 4:1.

	REC	OREC	a	b	c	HTCC
pH value	7.27	6.70	6.14	6.42	6.50	6.58
ζ-potential	−15.84	+24.53	+58.93	+60.02	+63.56	+66.06

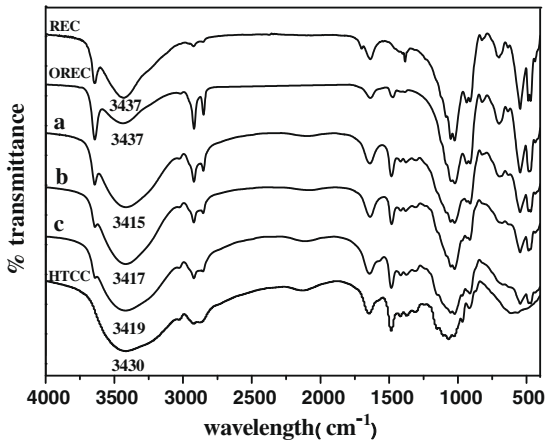

Fig. 3. FT-IR spectra of REC, OREC, HTCC and nanocompopsites with different HTCC/OREC ratios of (a) 1:1, (b) 2:1, and (c) 4:1.

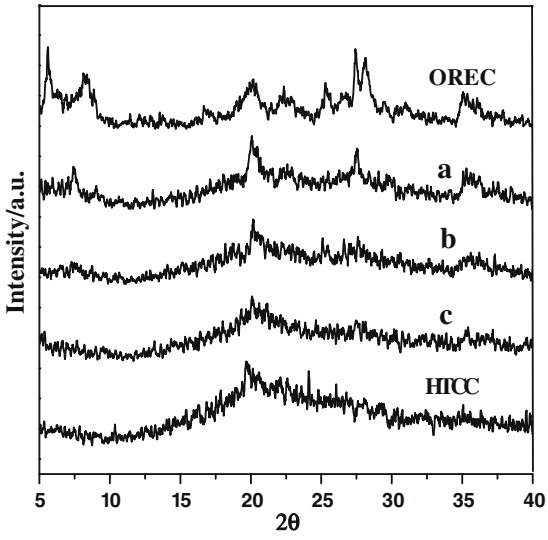

Fig. 4. XRD patterns of HTCC, OREC and nanocompopsites with different HTCC/OREC ratios of (a) 1:1, (b) 2:1 and (c) 4:1.

Table 2
MICs (%) (w/v) of nanocomposites comparing with HTCC, REC and OREC against different microorganisms in acetate buffer (pH 5.4), water and in pH 8.0.

Samples	Gram-positive bacteria						Gram-negative bacteria						Fungus		
	Staphylococcus aureus			*Bacillus subtilis*			*Escherichia coli*			*Pseudomonas aeruginosa*			*Aspergillus niveus*		
	pH 5.4	Water	pH 8.0	pH 5.4	Water	pH 8.0	pH 5.4	Water	pH 8.0	pH 5.4	Water	pH 8.0	pH 5.4	Water	pH 8.0
The blank	–	–	–	–	–	–	–	–	–	–	–	–	–	–	–
Acetate buffer	(0.1)*			-			(0.1)*			–			–		
Water		–			–			–			–			–	
NaOH solution			–			–			–			–			-
HTCC	0.05	0.1	0.1	0.05	0.1	0.1	0.1	0.1	0.1	0.1	-	-	0.1	-	-
REC	–	–	–	–	–	–	–	–	–	–	–	–	–	–	–
OREC	0.05	0.05	0.05	0.05	0.05	0.05	0.1	0.1	0.1	0.1	0.1	0.1	0.0125	0.0125	0.0125
HTCC/OREC nanocomposites (HTCC:OREC)															
1: 1	0.00313	0.00313	0.00313	0.00313	0.00313	0.00313	0.0125	0.025	0.05	0.1	0.1	0.1	0.00625	0.00625	0.0125
2: 1	0.00313	0.00313	0.00313	0.00313	0.00313	0.00625	0.0125	0.025	0.05	0.1	0.1	0.1	0.00625	0.00625	0.0125
4: 1	0.00313	0.00313	0.00313	0.00625	0.00625	0.00625	0.025	0.05	0.1	0.1	0.1	0.1	0.0125	0.0125	0.0125

"()": Ineffective at the tested concentration in brackets.
"-" : no inhibition result.

Table 3
Killing rate (%) of REC, OREC, HTCC and HTCC/OREC nanocomposites on microorganisms in different times.

Samples	*Staphylococcus aureus*					*Escherichia coli*				
	5 min	30 min	1 h	2 h	3 h	5 min	30 min	60 min	2 h	3 h
REC	–	–	–	–	–	–	–	–	–	–
OREC	17.8	29.6	35.5	46.7	60.6	15.2	26.4	33.5	39.8	52.5
HTCC	23.3	61.0	63.2	79.9	80.2	23.6	41.1	49.3	62.0	68.7
HTCC/OREC nanocomposites (HTCC:OREC)										
1:1	82.4	99.9	100	100	100	55.6	67.3	86.5	99.9	100
2:1	79.8	91.2	99.9	100	100	54.3	65.4	83.2	93.5	100
4:1	75.6	90.8	99.9	100	100	51.7	62.3	81.8	91.5	100

–, no inhibition result; e.g., growth rate of microorganism in sample plates was the same with that of control.

bial capacity in weak acid, water and even weak base, and the inhibitory actions are observed against a wide variety of microorganisms, including Gram-positive bacteria, Gram-negative bacteria and Fungi. The minimum inhibition concentration (MICs) values of the nanocomposites against Gram-positive bacteria are 8–32 times lower than that of HTCC; the MICs values against *E. coli* were only 2–8 times lower, and the MICs values against *A. niveus* also reach 8-16 times. Another *in vitro* antimicrobial assay (Table 3) showed that the nanocomposites can kill more than 90% of *S. aureus* and 80% of *E. coli* in 30 min, and can kill all bacteria in 3 h. The above results are agreement with the reported paper (Rhim et al., 2006), which reported that chitosan/organic clay nanocomposite films showed the good inhibitory property for the Gram-positive bacteria growth, but a little effect on Gram-negative bacteria. Compared to the chitosan-metal composites (Chen, Wu, & Zeng, 2005; Wang, Du, & Liu, 2004), the HTCC/OREC nanocomposites show better antimicrobial activity against Gram-positive bacteria, while a little weaker antimicrobial activity against Gram-negative bacteria. However, HTCC/OREC nanocomposites possess excellent antimicrobial activities in whichever medium. Therefore, they exhibit the potential in the biomedicine application in comparison with the CS-metal composites and our previous study (Wang et al., 2006).

Fig. 5 shows the TEM images of *E. coli* and *S. aureus* after treatment with buffer and the nanocomposites. It is obvious from the observations that bacteria change after two different treatments. *E. coli* turn from normal rod-shape to irregular shape after treatment with the nanocomposites. The cell walls of both strains are

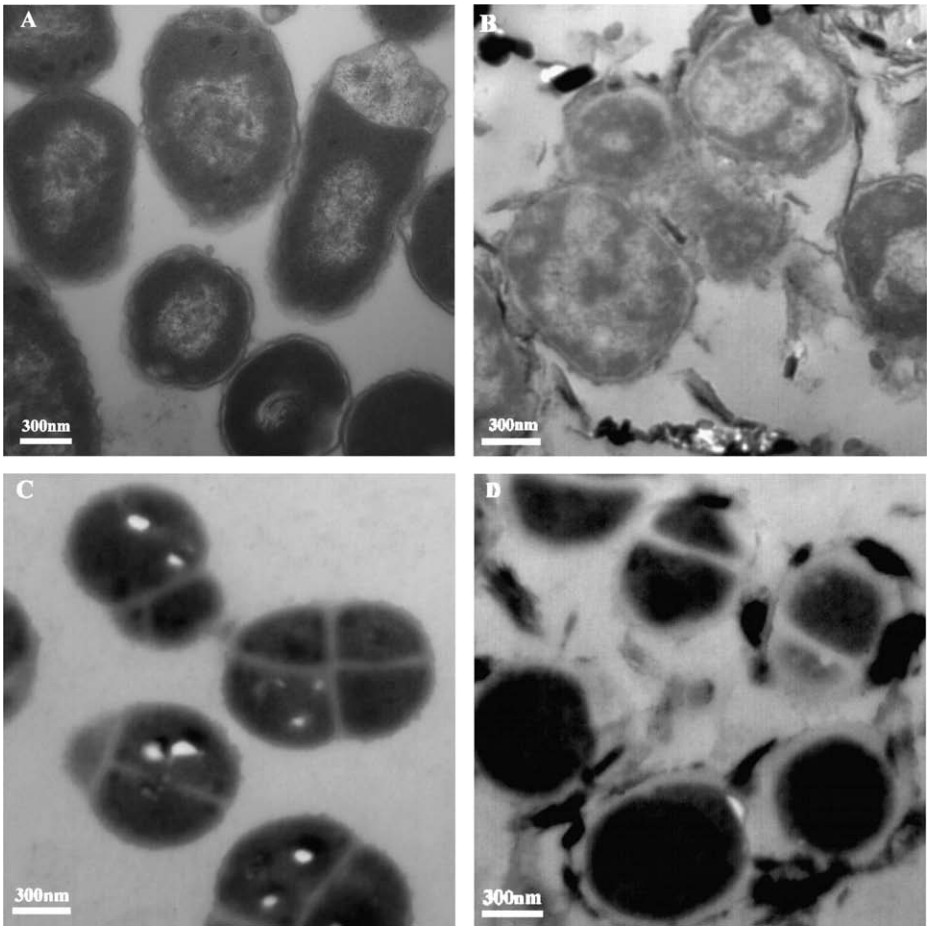

Fig. 5. TEM of E. coli (A) and S. aureus (C) cells after treatment with buffer, E. coli (B) and S. aureus (D) cells after treatment with the 0.05% (w/v) 1:1 HTCC/OREC nanocomposite acetate solution.

destroyed and become uneven. Moreover, the bacteria in fissive time are destroyed more seriously than those in mature period. More noticeably, some samples permeate into the cell.

It is well known that layered silicate can adhere to bacteria selectively (Xia, Hu, & Xu, 2005). Adsorption is the main interaction between silicate and bacteria. The adsorption effect is related to layer charge density of silicate. At physiological pHs, parent layered silicate exhibit a net negative charge (Nzengung, Voudrias, Nkedi-kissa, Wampler, & Weaver, 1996), as shown in Table 1. Under these conditions, negatively charged bacteria will not be significantly adsorbed onto these clays. However, clay surface will charge positively after modified by cationic materials as shown in Table 1. In this study, REC was firstly modified by CTAB and then intercalated by HTCC, thus materials with hydrophobicity and positive charge were produced. The positive charge of these intercalated clays may enhance their ability to adsorb bacteria through electrostatic interactions. In addition, there may be hydrophobic interaction between the hydrophobic alkyl chains of both HTCC and CTAB and lipophilic components of the bacterial cell walls, such as lipoproteins, liposaccharides and phospholipids (Zhang et al., 2003). Therefore, microorganisms in this system can be adsorbed and immobilized on the surface of the nanocomposites, and even the nanocomposites may enter into the cells (Fig. 5). In other words, the attraction of the bacteria to the silicate surface may be a vital important factor in the antimicrobial course. Evidence is as given in Tables 2 and 3, the 1:1 HTCC/OREC nanocomposite shows better inhibitory action against microorganisms than the 4:1 HTCC/OREC nanocomposite though they exhibit the similar Δd_L value. While the 1:1 HTCC/OREC nanocomposite exhibited similar antibacterial activity to the 2:1 HTCC/OREC nanocomposite although the former contains more amount of silicate than the later. The results indicate that the antimicrobial property is directly proportional to the amount or the interlayer distance of layered silicate, which is in agreement with our previous report (Wang et al., 2006). As the amount or the interlayer distance of clay increases, the effective layers in unit weight may increase owing to good dispersion (Fig. 2), thereupon larger specific surface area will be obtained, and more bacteria are adsorbed and immobilized on the surface of clay.

After quaternization, chitosan becomes a water-soluble polyelectrolyte with high charge density even at neutral pH values. The target site of this polycationic biocide is the negatively charged cell surface of the bacteria; it can interact and form polyelectrolyte complexes with polymers at the bacterial cell surface, which can change the permeability of the cell membrane of the microorganisms. This change may result in the leakage of proteinaceous and other intercellular components (Rabea, Badawy, Stevens, Smagghe, & Steurbaut, 2003), and then causes the death of the cell (Helander et al., 2001). Furthermore, this quaternary ammonium group can provide structure affinity between the cell surface of bacteria and HTCC, and disrupt the cell membranes of the microbes (Qin et al., 2004). Moreover, the long chain alkyls with hydrophobicity in HTCC can easily penetrate into the cell membrane (Liu et al., 2004). In this way, HTCC can exert strong inhibitory effect on growth of microorganisms. And importantly, it is soluble-water and thus shows antibacterial activity in weak acid, water and even weak base condition. Accordingly, HTCC/OREC nanocomposites can also disperse well in water, so they can also inhibit the growth of bacteria in weak acid, water and even weak base solution.

Based on the above analyses, the strong antimicrobial property may include two steps: the first step attributes to the adsorption and immobilization capacity of the bacteria from solution to the surface of REC by means of the hydrophobicity and positive charge of CTAB and HTCC; the second step is that HTCC can exert antimicrobial activity. Subsequently, HTCC/OREC nanocomposites can permeate into the cell membrane, damage the cell wall, disturb the natural processes of the cell and finally result in the death of microorganisms, especially against immature bacteria.

4. Conclusions

Novel organic/inorganic hybrid materials with strong antimicrobial activity were obtained by intercalation technique. The biopolymer (HTCC) entered into the interlayer of REC and nicely distributed in the HTCC matrix despite the high content of REC (25–50 wt %). It was the high affinity and the strong interaction between HTCC and REC that resulted in the excellent antimicrobial activity of the nanocomposites due to the adsorption and immobilization capacity of modified REC and the antimicrobial activity of HTCC. In these dual actions, the nanocomposites could permeate into the cell membrane, damage the cell wall, disturb the natural processes of the cell and finally result in the fast death of microorganisms. Such nontoxic and biocompatible nanocomposites combined the advantages of organic antimicrobial agents with inorganic antimicrobial agents, which will be valuable to the packaging and pharmaceutical application of polymer/layered silicate nanocomposites.

References

Chen, S. P., Wu, G. Z., & Zeng, H. Y. (2005). Preparation of high antimicrobial activity thiourea chitosan–Ag^+ complex. *Carbohydrate Polymers, 60*, 33–38.

Chen, P., & Zhang, L. N. (2006). Interaction and properties of highly exfoliated soy protein/montmorillonite nanocomposites. *Biomacromolecules,7*, 1700–1706.

Darder, M., Colilla, M., & Ruiz-Hitzky, E. (2003). Biopolymer-clay nanocomposites based on chitosan intercalated in montmorillonite. *Chemistry of Materials, 15*, 3774–3780.

Guo, T., Ma, Y. L., Guo, P., & Xu, Z. R. (2005). Antibacterial effects of the Cu (II)-exchanged montmorillonite on *Escherichia coli* K88 and *Salmonella choleraesuis*. *Veterinary microbiology, 105*, 113–122.

Helander, I. M., Nurmiaho-Lassila, E. L., Ahvenainen, R., Rhoades, J., & Roller, S. (2001). Chitosan disrupts the barrier properties of the outer membrane of Gram-negative bacteria. *International Journal of Food Microbiology, 71*, 235–244.

Herrera, P., Burghardt, R. C., & Phillips, T. D. (2000). Adsorption of *Salmonella enteritidis* by cetylpyridinium-exchanged montmorillonite clays. *Veterinary microbiology, 74*, 259–272.

Kotzle, A. F., Thanou, M. M., Lue, M., Xen, H. L., Boer, B. G., Verhoef, J. C., & Junginger, H. E. (1999). Effect of the degree of quaternization of N-trimethyl chitosan chloride on the permeability of intestinal epithelial cells (Caco-2). *European Journal of Pharmaceutics and Biopharmaceutics, 47*, 269–274.

Lemke, S. L., Grant, P. G., & Phillips, T. D. (1998). Adsorption of zearalenone by organophilic montmorillonite clay. *Journal of Agricultural and Food Chemistry, 46*, 3789–3796.

Li, H. B., Du, Y. M., Xu, X. J., & Zhan, H. Y. (2004). Effect of molecular weight and degree of substitution of quaternary chitosan on its adsorption and flocculation properties for potential retention-aids in alkaline papermaking. *Colloids and Surfaces A-Physicochemical Engineering Aspects, 242*, 1–8.

Liu, H., Du, Y. M., Wang, X. H., & Sun, L. P. (2004). Chitosan kills bacteria through cell membrane damage. *International Journal of Food Microbiology, 95*, 147–155.

Nzengung, V. A., Voudrias, E. A., Nkedi-kissa, P., Wampler, J. M., & Weaver, C. E. (1996). Organic cosolvent effects on sorption equilibrium of hydrophobic organic chemicals by organoclays. *Environmental Science and Technology, 30*, 89–96.

Qin, C. Q., Du, Y. M., & Xiao, L. (2002). Effect of hydrogen peroxide treatment on the molecular weight and structure of chitosan. *Polymer Degradation and Stability, 76*, 211–218.

Qin, C. Q., Xiao, Q., Li, H. R., Fang, M., Liu, Y., Chen, X., & Li, Q. (2004). Calorimetric studies of the action of chitosan-N-2-hydroxypropyl trimethyl ammonium chloride on the growth of microorganisms. *International Journal of Biological Macromolecules, 34*, 121–124.

Rabea, E. I., Badawy, M. E. T., Stevens, C. V., Smagghe, G., & Steurbaut, W. (2003). Chitosan as antimicrobial agent: Applications and mode of action. *Biomacromolecules, 4*, 1457–1465.

Ray, S. S., & Okamoto, M. (2003). Polymer/layered silicate nanocomposites: a review from preparation to processing. *Progress in Polymer Science, 28*, 1539–1641.

Rhim, J. W., Hong, S. I., Park, H. M., & Ng, P. K. W. (2006). Preparation and characterization of chitosan-based nanocomposite films with antimicrobial activity. *Journal of Agricultural and Food Chemistry, 54*, 5814–5822.

Shahidi, F., Arachchi, J. K. V., & Jeon, Y. J. (1999). Food applications of chitin and chitosans. *Trends in Food Science & Technology, 10*, 37–51.

Suci, P. A., Vrany, J. D., & Mittelman, M. W. (1998). Investigation of interactions between antimicrobial agents and bacterial biofilms using attenuated total reflection Fourier transform infrared spectroscopy. *Biomaterials, 19*, 327–339.

Vaia, R. A., Teukolsky, R. K., & Giannelis, E. P. (1994). Interlayer Structure and molecular environment of alkylammonium layered silicates. *Chemistry of Materials, 6*, 1017–1022.

Wang, X. H., Du, Y. M., & Liu, H. (2004). Preparation, characterization and antimicrobial activity of chitosan–Zn complex. *Carbohydrate Polymers, 56*, 21–26.

Wang, X. Y., Du, Y. M., Yang, J. H., Wang, X. H., Shi, X. W., & Hu, Y. (2006). Preparation, characterization and antimicrobial activity of chitosan/layered silicate nanocomposites. *Polymer,47*, 6738–6744.

Xia, M. S., Hu, C. H., & Xu, Z. R. (2005). Effects of copper bearing montmorillonite on the growth performance, intestinal microflora and morphology of weanling pigs. *Animal Feed Science and Technology, 118*, 307–317.

Xu, J., McCarthy, S. P., & Gross, R. A. (1996). Chitosan film acylation and effects on biodegradability. *Macromolecules, 29*, 3436–3440.

Zhang, Z. Q., Zhang, J., & Yu, H. X. (2003). Antibacterial effect of silver-carrying rectorite. *Wuhan University of Technology-Material Science Edition, 26*, 352–354.

Zhou, Y. H., Xia, M. S., Ye, Y., & Hu, C. H. (2004). Antimicrobial ability of Cu^{2+} - montmorillonite. *Applied Clay Science, 27*, 215–218.